Available online at www.sciencedirect.com
SCIENCE DIRECT®
Current Applied Physics 5 (2005) 213–217
Current Applied Physics
Physics, Chemistry and Materials Science
www.elsevier.com/locate/cap

Cross-platform characterization of electron tunneling in molecular self-assembled monolayers ☆

Takhee Lee *, Wenyong Wang, J.J. Zhang, J. Su, J.F. Klemic, M.A. Reed

Departments of Electrical Engineering, Applied Physics, and Physics, Yale University, P.O. Box 208284, New Haven, CT 06520, USA

Received 30 August 2003; accepted 7 November 2003
Available online 17 April 2004

Abstract

Electron tunneling is investigated for the alkanethiol self-assembled monolayers (SAMs) formed using three different device structures spanning from the nanometer to the micrometer scale. The measured current–voltage characteristics for the alkanethiol SAMs can be explained by the classical metal–insulator–metal tunneling model and the tunneling current exhibits overall exponential trend on the molecular length. Although different structures give consistent results (such as decay coefficient), unambiguous determination of the tunneling requires characterization of length and temperature dependencies.

PACS: 73.50.−h; 73.61.Ph; 73.40.Gk; 85.65.+h
Keywords: Self-assembled monolayer; Alkanethiol; Tunneling; Molecular electronics

1. Introduction

Characterization of charge transport in molecular scale electronic devices has to date shown exquisite sensitivity to specifics of device fabrication and preparation. Thus, intrinsic molecular band structure has been problematic to extract from published results. Here we investigate cross-platform device characterization through a large bandgap alkanethiol self-assembled monolayer (SAM) devices fabricated in different methods and platforms.

When a molecular layer with a large HOMO–LUMO gap (HOMO: highest occupied molecular orbital, LUMO: lowest unoccupied molecular orbital) is sandwiched between two metal contacts, a well-defined metal–insulator–metal (M–I–M) tunneling is expected. One molecular system that has been studied extensively is the alkanethiol [$CH_3(CH_2)_{n-1}SH$] SAM [1]. Scanning tunneling microscopy [2], conducting atomic force microscopy (CAFM) [3,4], mercury-drop junctions [5,6], and cross-wire junctions [7] have been used to investigate electron transport through alkanethiol SAMs. The electron conduction through alkanethiol SAMs is expected to be tunneling because the Fermi levels of the contacts lie within the large HOMO–LUMO gap (~8 eV) of short molecular length (1–2.5 nm) for the case of these alkanethiols [8]. Although it has been recently shown that tunneling is the main conduction mechanism through the alkanethiol SAMs from temperature-independent current–voltage [$I(V)$] measurement results [8], the tunneling current densities and the electrical parameters determining the tunneling characteristics such as the tunneling barrier height and the decay coefficient vary among the different measurement techniques [2–6,8] which can be due to different geometry, junction area uncertainty, and device-to-device variation.

In this study, tunneling characteristics through alkanethiol SAMs are investigated using three types of device structures: nanometer scale and micrometer scale device structures and a structure for CAFM study. The measured $I(V)$ data are compared with theoretical calculations of the M–I–M tunneling model. $I(V)$ measurements on various alkanethiols of different molecular

☆ Original version presented at the 4th International Conference on Electroluminescence of Molecular Materials and Related Phenomena (ICEL4), 27–30 August 2003, Cheju Island, Korea.

* Corresponding author. Address: Department of Materials Science and Engineering, Kwangju Institute of Science and Technology, 1 Oryong-dong, Buk-gu, Kwangju 500-712, South Korea. Tel.: +82-62-970-2302; fax: +82-62-970-2304.
E-mail address: tlee@kjist.ac.kr (T. Lee).

1567-1739/$ - see front matter © 2004 Elsevier B.V. All rights reserved.
doi:10.1016/j.cap.2003.11.088

lengths are also performed for the study of length-dependent tunneling behavior.

2. Experimental

2.1. Alkanethiol deposition

For our experiments, $a \sim 5$ mM alkanethiol solution was prepared by adding ~10 μl alkanethiols into 10 ml ethanol. The deposition was done in solution for 1–2 days inside nitrogen filled glove box with an oxygen level of less than 100 ppm (or 1 ppm). Alkanethiols of different molecular lengths: octanethiol [$CH_3(CH_2)_7SH$; denoted as C8, for the number of alkyl units], decanethiol [$CH_3(CH_2)_9SH$; C10], dodecanethiol [$CH_3(CH_2)_{11}SH$; C12], tetradecanethiol [$CH_3(CH_2)_{13}SH$; C14], hexadecanethiol [$CH_3(CH_2)_{15}SH$; C16] were used to form the active molecular component. As a representative example, the chemical structure of octanethiol is shown in Fig. 1(a).

2.2. Device fabrication

Electrical transport measurements on alkanethiol SAMs were performed using three types of nanoscale or microscale device structures, as schematically illustrated in Fig. 1. The first type [Fig. 1(a)] is a nanoscale device structure, similar to one reported previously [9]. The average diameter of device size [circled in Fig. 1(a)] was determined to be ~45 nm from scanning electron microscope (SEM) images [8]. The second type [Fig. 1(b)] is a microscale device structure fabricated by conventional microlithography. The junction diameter of the microscale devices was determined as 960 ± 60 nm from AFM images on various devices.

For these two types of devices, after alkanethiol SAMs were formed on the exposed Au surfaces, the other Au contact (~100 nm Au) was made by thermal evaporation (under the pressure of $\sim 10^{-8}$ Torr) while liquid nitrogen was kept flowing through the cooling stage in order to avoid thermal damage to the molecular layer [8,10]. The devices were then subsequently packaged and loaded into a Janis cryostat. Variable temperature two-terminal $I(V)$ measurements were performed using semiconductor parameter analyzer (HP4145B or Agilent 4156B).

Alkanethiol SAMs were also deposited on the third type of device structure [Fig. 1(c)]: atomically flat Au surfaces (Au/Cr/glass) prepared by hydrogen flame annealing. The CAFM technique [3,4] was utilized to perform the $I(V)$ measurements on this structure at room temperature in ambient environment, as illustrated in

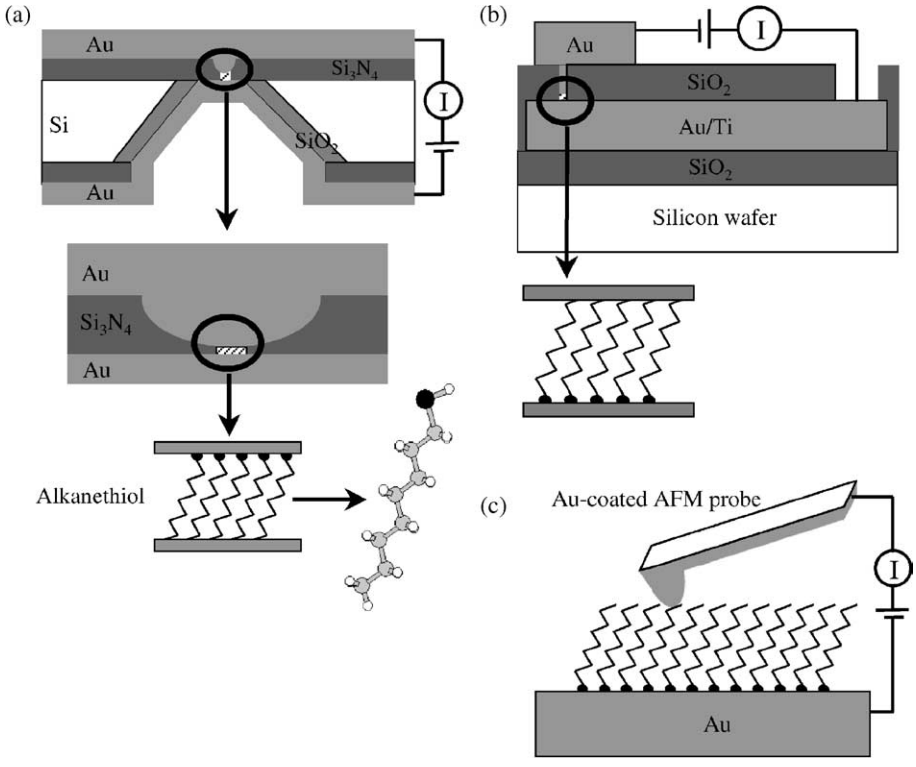

Fig. 1. Schematics of three types of device structures used in this study. (a) Nanoscale device. Top schematic is the cross-section of a silicon wafer with a nanometer scale pore etched through a suspended silicon nitride membrane. Middle and bottom schematics show a Au/SAM/Au junction (area ~45 nm in diameter) formed in the pore area. The structure of octanethiol is shown as an example. (b) Microscale device structures. The junction area is ~960 nm in diameter. (c) Schematics illustrating conducting atomic force microscopy study on alkanethiol SAMs formed on atomically flat Au surface.

Fig. 1(c) [11]. CAFM $I(V)$ measurements were performed using an external electronic unit (HP4145B semiconductor parameter analyzer) by connecting it to the conducting AFM probe and the sample in study.

3. Results

3.1. Method 1. Nanoscale devices

Fig. 2 shows representative $I(V)$ characteristics of C8, C12, and C16 SAMs measured (symbols) with the device structure as shown in Fig. 1(a). By using the contact area of 45 ± 2 nm (for C12 and C16 devices) [8] and 50 ± 8 nm (for C8 device) in diameter, current densities of $31{,}000 \pm 10{,}000$, 1500 ± 200, and 23 ± 2 A/cm^2 at 1.0 V are determined for C8, C12, and C16, respectively. From the temperature-independent current–voltage measurement results, tunneling was shown to be the main conduction mechanism occurring through alkanethiol SAMs, as seen for M–I–M tunneling [8]. The simplest model to describe the M–I–M tunneling characteristics is the Simmons model [12,13]. The Simmons model expresses the tunneling current density through a barrier in the tunneling regime as [5,8,12]

$$J = \left(\frac{e}{4\pi^2\hbar d^2}\right)\left\{\left(\Phi_B - \frac{eV}{2}\right) \times \exp\left[-\frac{2(2m)^{1/2}}{\hbar}\alpha\left(\Phi_B - \frac{eV}{2}\right)^{1/2} d\right] - \left(\Phi_B + \frac{eV}{2}\right) \times \exp\left[-\frac{2(2m)^{1/2}}{\hbar}\alpha\left(\Phi_B + \frac{eV}{2}\right)^{1/2} d\right]\right\}, \quad (1)$$

where m is electron mass, d is barrier width, Φ_B is barrier height, V is the applied bias, h $(= 2\pi\hbar)$ is Planck's constant, and α is a unitless adjustable parameter that is introduced to modify the simple rectangular barrier model or to account for an effective mass [5,8]. $\alpha = 1$ corresponds to the case for a rectangular barrier and bare electron mass, and has been previously shown not to fit $I(V)$ data well for some alkanethiol measurements [5].

From Eq. (1) by adjusting two parameters Φ_B and α, a nonlinear least square fitting can be performed to fit the measured $I(V)$ data. The best fitting parameters (minimized χ^2) for the $I(V)$ data were found to be $\{\Phi_B = 1.83 \pm 0.10$ eV and $\alpha = 0.61 \pm 0.01\}$, $\{\Phi_B = 1.42 \pm 0.04$ eV and $\alpha = 0.65 \pm 0.01\}$, and $\{\Phi_B = 1.40 \pm 0.03$ eV and $\alpha = 0.68 \pm 0.01\}$ for C8, C12, and C16 $I(V)$ data, respectively, where the error ranges of Φ_B and α are dominated by potential device size fluctuations. These calculation results are plotted as solid curves in Fig. 2.

The physical meaning of α provides a way of applying the tunneling model of a rectangular barrier to tunneling either through a nonrectangular barrier [5], a proposed effective mass (m^*) of the tunneling electrons through the molecules [4,8,14], or a combination of both. m^* $(= \alpha^2)$ corresponds to 0.37, 0.42, and 0.46 m for C8, C12, and C16, respectively from the obtained α values.

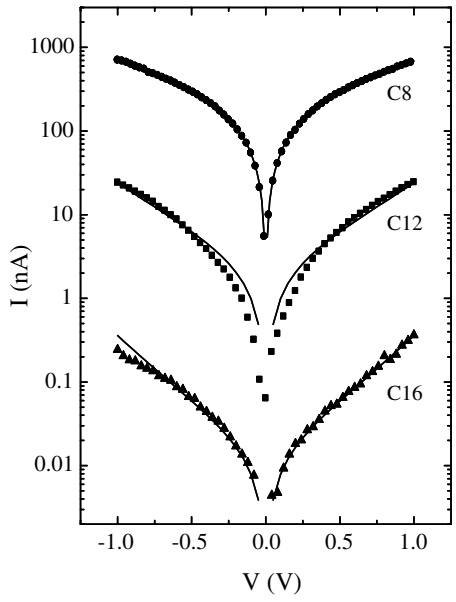

Fig. 2. $I(V)$ characteristics of C8, C12, and C16 SAMs formed on device structure shown in Fig. 1(a). Measured data (symbols) are compared with calculations (solid curves) using the optimum fitting parameters of Φ_B and α (see text).

The conductance of tunneling characteristics through alkanethiol SAMs is exponentially dependent on the barrier width d as [2–6,8,15]

$$G \propto \exp(-\beta d), \quad (2)$$

where β is a decay coefficient that is a bias-dependent quantity [8,16]. Fig. 3(a) is a log plot of tunneling current densities at various voltages as a function of the molecular length (tunneling barrier width) for these alkanethiols. The molecular lengths used in this plot are 13.3, 18.2, and 23.2 Å for C8, C12, and C16, respectively (each molecular length was determined by adding an Au-thiol bonding length to the length of molecule). Note that these lengths implicitly assume "through-bond" tunneling, that is, along the tilted molecular chains between the metal contacts [3].

As seen in Fig. 3(a), the tunneling current densities show exponential dependence on molecular length. The β values can be determined from the slope at each bias and are plotted in Fig. 3(b). This gives a β value from 0.84 to 0.73 Å^{-1} in the bias range from 0.1 to 1.0 V. β value decreases as bias increases especially when bias becomes larger than 0.5 V, which results from barrier lowering effect due to the applied bias. As shown previously, the β values are almost independent of bias in the low bias range (especially $V <\sim 0.5$ V) [8], which gives an average $\beta = 0.83 \pm 0.04$ Å^{-1} in the low bias region (from 0 to 0.5 V) from Fig. 3(b).

The β values for alkanethiols obtained by various experimental techniques have previously been reported

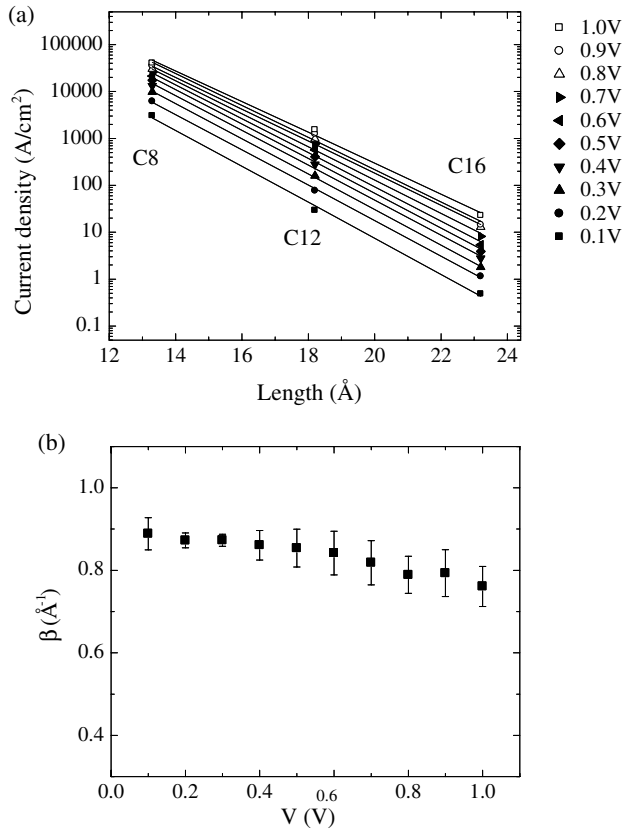

Fig. 3. (a) Log plot of tunneling current densities for nanoscale alkanethiol SAM devices as a function of molecular lengths. The lines through the data points are exponential fittings. (b) Plot of β versus bias.

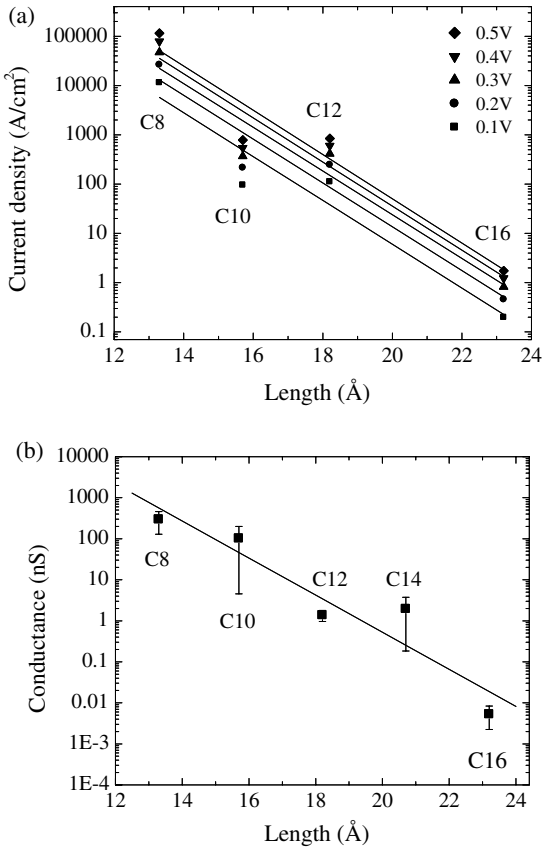

Fig. 4. (a) Log plot of tunneling current densities for microscale alkanethiol SAM devices as a function of molecular lengths. It is plotted in the same scale as in Fig. 3(a) for comparison. The lines through the data points are exponential fittings. (b) Log plot of conductance of alkanethiol SAMs formed on CAFM device structure as a function of molecular lengths (at $F = 20$ nN). The line through the data points is exponential fitting.

[2–6,8]. For example, Holmlin et al. reported a β value of 0.87 Å^{-1} by mercury-drop experiments [5], and Wold et al. reported β of 0.94 Å^{-1} and Cui et al. reported β of 0.64 Å^{-1} for various alkanethiols by using the CAFM technique [3,4].

3.2. Method 2. Microscale devices

Fig. 4(a) is a log plot of tunneling current densities at various voltages as a function of the molecular length for the alkanethiol devices fabricated in the microscale device structure as shown in Fig. 1(b). It is plotted in the same scale as in Fig. 3(a) for comparison. The current densities were estimated using the junction area of 960 ± 60 nm in diameter, and determined to be 115,000 ± 14,000 (at 0.5 V), 3300 ± 400 (at 1.0 V), and 6.6 ± 0.8 (at 1.0 V) A/cm^2 for C8, C12, and C16, respectively [17]. The current densities estimated in this structure in the same order of magnitude from those observed in the previous structure (nanoscale device) within a factor 2–9 difference. The current density of C10 device has been observed smaller than that of C12 device, which is attributed to the device-to-device variation in the microscale devices or the discrepancy of SAM quality (defects or grain boundaries) between in the nanometer and micrometer scales. With the exception for C10 device result, the tunneling current densities show exponential trend on the molecular length, which gave bias-independent β value of 1.0 ± 0.2 Å^{-1} in the bias range of 0–0.5 V. The bias-dependence of β appears only at high bias range [8] [see Fig. 3(b)]. The observed β value here are consistent with that observed in the method 1, although the agreement may be fortuitous. The large uncertainty in β value reflects the dispersion in current densities for various alkanethiols and problems with this method.

Although it was shown that the tunneling is the main mechanism for alkanethiol SAMs in the nanoscale devices [8], alkanethiol SAMs in the microscale devices may contain more significant defects than in the nanoscale devices, thus other conduction mechanism especially defect-mediated transport [18,19] cannot be ruled out. Temperature-dependent $I(V)$ measurements (which have not yet been successfully performed in this type of device) are critical to unambiguously claim tunneling and accurate β values.

3.3. Method 3. CAFM study

Fig. 4(b) is a log plot of the conductance measured by the CAFM technique as a function of the molecular length for different alkanethiols for $F = 20$ nN [20]. The conductance was obtained from linear fitting of $I(V)$ data in low bias regime, typically $V < |0.5|$ V. The conductance values are in good agreement with the values reported from the previous CAFM studies by Wold et al. [3]. The conductance also shows overall exponential trend on molecular length. The line through the data points is exponential fitting with the error range determined as standard deviation of the measured resistance values at different locations. The β value was determined as 1.04 ± 0.20 Å^{-1} from the slope of the exponential fitting. This β value is also consistent with those observed in the two previous methods. However, the tip loading force may cause penetration and/or deformation of the SAMs and the role of absorbates (such as water) in the molecule-tip junction has not been quantified, which makes this method less controlled and prone to systematic errors. Here, variable temperature measurements (to determine the contribution due to defects) are problematic, again showing the results can be consistent but are not unambiguous.

4. Conclusions

Electron tunneling through alkanethiol SAMs was investigated using three different structures. The tunneling conduction was examined by varying molecular length. Although all the three structures showed exponential dependence on the molecular length with a decay coefficient, alkanethiol SAMs formed in the nanometer scale structure were the only ones in which tunneling transport is unambiguously shown; i.e., temperature-independent and length-dependent conduction. Although other methods can give consistent results, unambiguous determination of the tunneling transport mechanism requires the characterization of length and temperature dependencies.

Acknowledgements

The authors would like to thank Ilona Kretzschmar, Azucena A. Munden, and Ryan Munden for helpful discussions. This work was supported by DARPA/ONR (N00014-01-1-0657), ARO (DAAD19-01-1-0592), AFOSR (F49620-01-1-0358), NSF (DMR-0095215), and NASA (NCC2-1363).

References

[1] A. Ulman, An Introduction to Ultrathin Organic Films from Langmuir–Blodgett to Self-Assembly, Academic Press, 1991.
[2] L.A. Bumm, J.J. Arnold, T.D. Dunbar, D.L. Allara, P.W. Weiss, J. Phys. Chem. B 103 (1999) 8122.
[3] D.J. Wold, R. Haag, M.A. Rampi, C.D. Frisbie, J. Phys. Chem. B 106 (2002) 2813.
[4] X.D. Cui, X. Zarate, J. Tomfohr, O.F. Sankey, A. Primak, A.L. Moore, T.A. Moore, D. Gust, G. Harris, S.M. Lindsay, Nanotechnology 13 (2002) 5.
[5] R. Holmlin, R. Haag, M.L. Chabinyc, R.F. Ismagilov, A.E. Cohen, A. Terfort, M.A. Rampi, G.M. Whitesides, J. Am. Chem. Soc. 123 (2001) 5075.
[6] R.L. York, P.T. Nguyen, K. Slowinski, J. Am. Chem. Soc. 125 (2003) 5948.
[7] J.G. Kushmerick, D.B. Holt, S.K. Pollack, M.A. Ratner, J.C. Yang, T.L. Schull, J. Naciri, M.H. Moore, R. Shashidhar, J. Am. Chem. Soc. 124 (2002) 10654.
[8] W. Wang, T. Lee, M.A. Reed, Phys. Rev. B 68 (2003) 035416.
[9] C. Zhou, M.R. Deshpande, M.A. Reed, L. Jones II, J.M. Tour, Appl. Phys. Lett. 71 (1997) 611.
[10] R.M. Metzger, B. Chen, U. Ho1pfner, M.V. Lakshmikantham, D. Vuillaume, T. Kawai, X. Wu, H. Tachibana, T.V. Hughes, H. Sakurai, J.W. Baldwin, C. Hosch, M.P. Cava, L. Brehmer, G.J. Ashwell, J. Am. Chem. Soc. 119 (1997) 10455.
[11] AFM system used in this study is ThermoMicroscope (CP-Research model) ambient AFM/STM system from Veeco Instruments Inc.
[12] J.G. Simmons, J. Appl. Phys. 34 (1963) 1793.
[13] Franz two-band model can also explain the alkanethiol tunneling characteristics. See Ref. [8].
[14] C. Joachim, M. Magoga, Chem. Phys. 281 (2002) 347.
[15] M.P. Samanta, W. Tian, S. Datta, J.I. Henderson, C.P. Kubiak, Phys. Rev. B 53 (1996) 7626.
[16] Note that the β values obtained using Eqs. (1) and (2) are slightly different. See Ref. [8].
[17] The C8 device degraded due to the large current level (>∼mA) when a higher bias (> – 0.5 – V) was applied. C14 devices have not been successfully fabricated.
[18] B. Mann, H. Kuhn, J. Appl. Phys. 42 (1971) 4398.
[19] E.E. Polymeropoulos, J. Sagiv, J. Chem. Phys. 69 (1978) 1836.
[20] The CAFM probe is Au (20 nm)/Cr (20 nm) coated AFM probe purchased from MicroMasch (http://www.spmtips.com/). Its nominal force constant is 0.35 N/m. The radius of the probe end is ∼90 nm determined from SEM images.